Phenological changes of oceanic phytoplankton in the 1980s and 2000s as revealed by remotely sensed ocean-color observations

Fabrizio d'Ortenzio, David Antoine, Elodie Martinez, Maurizio Ribera d'Alcala

▶ **To cite this version:**

Fabrizio d'Ortenzio, David Antoine, Elodie Martinez, Maurizio Ribera d'Alcala. Phenological changes of oceanic phytoplankton in the 1980s and 2000s as revealed by remotely sensed ocean-color observations. Global Biogeochemical Cycles, 2012, 26, pp.GB4003,. 10.1029/2011GB004269 . hal-00747089

HAL Id: hal-00747089
https://hal.science/hal-00747089

Submitted on 9 Apr 2021

HAL is a multi-disciplinary open access archive for the deposit and dissemination of scientific research documents, whether they are published or not. The documents may come from teaching and research institutions in France or abroad, or from public or private research centers.

L'archive ouverte pluridisciplinaire **HAL**, est destinée au dépôt et à la diffusion de documents scientifiques de niveau recherche, publiés ou non, émanant des établissements d'enseignement et de recherche français ou étrangers, des laboratoires publics ou privés.

Phenological changes of oceanic phytoplankton in the 1980s and 2000s as revealed by remotely sensed ocean-color observations

Fabrizio D'Ortenzio,[1,2] David Antoine,[1,2] Elodie Martinez,[1,2,3] and Maurizio Ribera d'Alcalà[4]

Received 29 November 2011; revised 28 August 2012; accepted 4 September 2012; published 12 October 2012.

[1] We investigated the phenology of oceanic phytoplankton at large scales over two 5-year time periods: 1979–1983 and 1998–2002. Two ocean-color satellite data archives (Coastal Zone Color Scanner (CZCS) and Sea-viewing Wide Field-of-view Sensor (SeaWiFS)) were used to investigate changes in seasonal patterns of concentration-normalized chlorophyll. The geographic coverage was constrained by the CZCS data distribution. It was best for the Northern Hemisphere and also encompassed large areas of the Indian, South Pacific, and Equatorial Atlantic regions. For each 2° pixel, monthly climatologies were developed for satellite-derived chlorophyll, and the resulting seasonal cycles were statistically grouped using cluster analysis. Five distinct groups of mean seasonal cycles were identified for each half-decade period. Four types were common to both time periods and correspond to previously identified phytoplankton regimes: Bloom, Tropical, Subtropical North, and Subtropical South. Two other mean seasonal cycles, one in each of the two compared 5-year periods, were related to transitional or intermediate states (Transitional Tropical and Transitional Bloom). Five mean seasonal cycles (Bloom, Tropical, Subtropical North, and Subtropical South, Transitional Bloom) were further confirmed when the whole SeaWiFS data set (1998–2010) was analyzed. For ∼35% of the pixels analyzed, characteristic seasonal cycles of the 1979–1983 years differed little from those of the 1998–2002 period. For ∼65% of the pixels, however, phytoplankton seasonality patterns changed markedly, especially in the Northern Hemisphere. Subtropical regions of the North Pacific and Atlantic experienced a widespread expansion of the Transitional Bloom regime, which appeared further enhanced in the climatology based on the full SeaWiFS record (1998–2010), and, as showed by a more detailed analysis, is associated to La Niña years. This spatial pattern of Transitional Bloom regime reflects a general smoothing of seasonality at macroscale, coming into an apparent greater temporal synchrony of the Northern Hemisphere. The Transitional Bloom regime is also the result of a higher variability, both in space and time. The observed change in phytoplankton dynamics may be related not only to biological interactions but also to large-scale changes in the coupled atmosphere–ocean system. Some connections are indeed found with climate indices. Changes were observed among years belonging to opposite phases of ENSO, though discernible from the change among the two periods and within the SeaWiFS era (1998–2010). These linkages are considered preliminary at present and are worthy of further investigation.

Citation: D'Ortenzio, F., D. Antoine, E. Martinez, and M. Ribera d'Alcalà (2012), Phenological changes of oceanic phytoplankton in the 1980s and 2000s as revealed by remotely sensed ocean-color observations, *Global Biogeochem. Cycles*, *26*, GB4003, doi:10.1029/2011GB004269.

1. Introduction

[2] Phenology is the study of naturally recurring events [*Menzel et al.*, 2006], such as the onset of spring bird nesting, the timing of bears' winter lethargy, or the length of the summer growing season. Such studies have long been used to describe terrestrial ecosystems and infer forcing mechanisms [*Cleland et al.*, 2007; *Penuelas et al.*, 2009], but phenological patterns and dependencies are much less well characterized for ocean ecosystems. Freshwater and coastal phytoplankton phenologies are also relatively well documented compared to those of the open ocean [*Huber*

[1]Laboratoire d'Océanographie de Villefranche, CNRS, UMR 7093, Villefranche-sur-Mer, France.
[2]Pôle Terre vivante et environnement, Université Pierre et Marie Curie, Paris, France.
[3]Now at Mediterranean Institute of Oceanography, Aix-Marseille University, Marseille, France.
[4]Stazione Zoologica Anton Dohrn Napoli, Naples, Italy.

Corresponding author: F. D'Ortenzio, Laboratoire d'Océanographie de Villefranche, CNRS, UMR 7093, BP 8, Quai de la Darse, F-06238 Villefranche-sur-Mer, France. (dortenzio@obs-vlfr.fr)

©2012. American Geophysical Union. All Rights Reserved.
0886-6236/12/2011GB004269

et al., 2008; *Kromkamp and Van Engeland*, 2010; *Winder and Schindler*, 2004].

[3] Evolution of marine biota under changing environmental conditions—at interannual, decadal, and longer time scales—remains a poorly understood phenomenon. Phenological analysis offers a valuable approach to characterizing phytoplankton seasonal cycles and their relation to environmental changes. Such characterizations are central to disentangling the complicated cause–effect relationships between climate forcing and phytoplankton response, and in turn improving numerical predictions of ecosystem response to future climate scenarios [*Sarmiento et al.*, 2004].

[4] One reason that pelagic phytoplankton phenology has remained a major challenge [*Edwards and Richardson*, 2004] is the difficulty of obtaining continuous observations throughout an annual cycle. With the growing availability of biological ocean time series, phenological studies of oceanic phytoplankton are receiving increasing attention [*Ji et al.*, 2010]. Relevant open-ocean findings have been recently reported from analyses of in situ and satellite data [*Beaugrand et al.*, 2009; *Beaugrand et al.*, 2002; *Behrenfeld et al.*, 2005; *Boyce et al.*, 2010; *Conkright and Gregg*, 2003; *Edwards and Richardson*, 2004; *Gregg et al.*, 2003; *Racault et al.*, 2012].

[5] Satellite ocean color observations, in particular, show strong promise for providing empirical time series data with the temporal and spatial resolution needed to characterize phytoplankton phenology at regional and global scales. Such data sets have been previously used to characterize biogeochemical provinces and major phenological events for phytoplankton over large areas of the oceans [*Devred et al.*, 2007; *Henson et al.*, 2009; *Platt and Sathyendranath*, 2008; *Platt et al.*, 2010; *Platt et al.*, 2009; *Siegel et al.*, 2002]. Satellite observations are limited to characterizations of the surface ocean, but as noted by *Ji et al.* [2010], their synopticity, global coverage, and relatively high temporal frequency provide compensating benefits. Satellite data provide a powerful tool for investigating phytoplankton phenological patterns [*Platt et al.*, 2009].

[6] Most previous analyses of satellite ocean-color observations have focused on phytoplankton blooms, which have been typically considered to be the primary phenological feature for phytoplankton [i.e., *Racault et al.*, 2012]. Also worthy of investigation are areas lacking conspicuous bloom events (e.g., tropical regions), as well as periods of the year when phytoplankton biomass displays only small changes. Key stages of phytoplankton temporal evolution, such as bloom decay or secondary blooming events, have been generally overlooked [but see *Vargas et al.*, 2009].

[7] In this work, we address this gap by using satellite ocean color observations to characterize phytoplankton phenological traits for whole seasonal cycles over large oceanic areas. We explored the possibility offered by a recently generated ocean color data set to investigate whether the oceanic phytoplankton phenology displayed changes over relatively long periods. High quality ocean color global data have been routinely collected since 1997 [*McClain*, 2009], when the first new generation ocean color mission started with the Sea-viewing Wide Field-of-view Sensor (SeaWiFS). However, the first ocean color mission was the Coastal Zone Color Scanner (CZCS), which generated, from 1978 to 1986, the first global data set of ocean color observations [*Hovis et al.*, 1980]. Although less technologically advanced than the present-day sensors, the CZCS produced a set of crucial observations, which provided the first characterization of the global scale spatiotemporal variability of the oceanic surface chlorophyll [*Longhurst*, 1995]. Despite the difference in sensor design and performance, the homogenization of the CZCS and the SeaWiFS observations (for the years 1979–1983 and for the period 1998–2002, respectively) has been accomplished [*Antoine et al.*, 2005]. This data set was obtained by processing CZCS and SeaWiFS observations with strictly identical algorithms. Therefore, this data set is appropriate to detect possible phenological changes over two periods separated by 20 years, and to explore their possible links and feedbacks with the environmental forcing.

[8] The first aim of the paper is then to exploit the new CZCZ/SeaWiFS data set to identify possible modifications of the main patterns of the global scale phytoplankton phenology, over the two periods 1979–1983 and 1998–2002. The similarities and the differences observed over these two periods provide preliminary insights about the changing characteristics of the phytoplankton phenology over a long time frame. The relatively narrow temporal windows of the two series prevent a full assessment of trends or biases, however. Nevertheless, phenological characteristics resulting from the comparison of the two 5-years periods provide a first guess of possible changes, which could facilitate other approaches in identifying long-term changes, if any. The results of our analysis also provide an experimentally derived framework to modeling approaches, which represent the key scientific tool to reconstruct ocean dynamic when data are missing (i.e., short-term or sporadic observations are often used to constraint long-term simulations; see, for example, *Henson et al.* [2009]).

[9] In this study, phenological phytoplankton patterns are elucidated by a novel approach based on cluster analysis, which has been tested at a regional scale for the Mediterranean Sea [*D'Ortenzio and Ribera d'Alcalà*, 2009]. This approach allows for the identification of a limited number of seasonal-cycle types considered to be statistically representative of the initial data set. The spatial distributions of the seasonal cycles are then mapped for each time period, as are the 20-year differences. We also analyze the entire SeaWiFS time series (1998–2010) and compare it to the SeaWiFS 5 year time series (1998–2002) to assess possible biases due to subsampling of long-term changes when using only 5-year averages. We also map 20-year differences in mixed layer characteristics—specifically, annual maxima and timing of the annual maxima. Finally, we explore possible linkages between changes in phenology and changes in climate indices that track large-scale ocean–atmosphere phenomena, such as the Atlantic Multidecadal and Pacific Decadal Oscillations (AMO and PDO) and El Niño–Southern Oscillation (ENSO) events. To better elucidate the ENSO effect on phytoplankton phenology, we also carried out the analysis of the whole SeaWiFS data set (1998–2010), by separately grouping the El Niño and La Niña years.

2. Data and Methods

2.1. Satellite Data

[10] Ocean color time series are provided by the CZCS [*Hovis et al.*, 1980] and the SeaWiFS, [*McClain et al.*, 2004] missions. Caution is required when comparing data from

these two time series, which are separated by an 11-year gap and cannot be cross-validated. We used the reprocessed data set generated by *Antoine et al.* [2005], who applied the same algorithms and an adapted calibration to both CZCS and SeaWiFS observations to yield two fully compatible 5-year time series of chlorophyll (Chl) concentration data. Readers are referred to *Antoine et al.* [2005] for further explanation of this reprocessing and to *Martinez et al.* [2009] for an illustration of how these data sets have been used to quantitatively analyze basin-scale phytoplankton changes over twenty years.

[11] The years 1979 to 1983 were selected for the CZCS analyses because few data are available from 1984 and calibration is uncertain for 1985 and 1986. The reprocessed SeaWiFS data set, which was generated in 2003 from the standard NASA Level-1a products (i.e., raw data), includes the five years from 1998 to 2002. The full SeaWiFS record (1998–2010) was used in the version distributed by the NASA (reprocessing #5). A comparison between the NASA standard and the reprocessed SeaWiFS products was presented in *Antoine et al.* [2005]. The existing differences between the two archives show very weak seasonal variability, ensuring that if normalized data are used instead of absolute values, the two products are comparable.

[12] We initially remapped the *Antoine et al.* [2005] 5-year climatological data (for the periods 1979–1983 and 1998–2002) at a 2° spatial resolution, retaining only those pixels that had a full set of twelve monthly mean Chl values for both the data sets (i.e., the resulting two climatologies have the same number of pixels, and every pixel has a full year of monthly mean CZCS Chl values and a full year of monthly mean SeaWiFS Chl). Coastal areas with water depth <200 m were excluded. Because CZCS observations were intermittent in the Southern Hemisphere, the data sets generated for the periods 1979–1983 and 1998–2002 cover essentially the Northern Hemisphere between 10° and 40°N with partial coverage up to 50°N, plus a few regions of the Southern Hemisphere (i.e., the western Indian Ocean, the southwestern Pacific, and the western equatorial Atlantic). This spatial distribution was also imposed on the full SeaWiFS record (1998–2010), and a climatology with the same characteristics of the 1979–1983 and 1998–2002 climatologies (monthly, 2° resolutions) was then generated.

[13] For each pixel and each climatology, the twelve monthly chlorophyll concentrations normalized by the maximum observed Chl concentration. (For a detailed description of the normalization method, see *D'Ortenzio and Ribera d'Alcalà* [2009].)

[14] Note that the normalization imposed on the three data sets (1979–1983, 1998–2002 and 1998–2010) emphasizes the shapes of the seasonal cycles rather than the absolute values of the chlorophyll concentrations. It minimizes also the effects of possible remaining bias between the three data sets.

[15] In the following, we refer to the *Antoine et al.* [2005] reprocessed data sets as the "1979–1983" and "1998–2002" data and to the standard full SeaWiFS data sets as "1998–2010" data.

2.2. Cluster Analysis

[16] The cluster-analysis method used here was initially developed to identify phenological traits of the Mediterranean Sea from time series of SeaWiFS chlorophyll concentrations [*D'Ortenzio and Ribera d'Alcalà*, 2009]. Similar techniques are routinely used in the atmospheric sciences [*Fovell*, 1997; *Lund and Li*, 2009]. The cluster analysis was applied to the normalized remotely sensed chlorophyll concentrations. This technique groups sites (pixels in satellite fields) that exhibit similarly shaped seasonal cycles—i.e., similar phenologies. The center (average cycle) within each group or cluster is then computed to provide a single characteristic seasonal cycle that is statistically representative of the group as a whole (depending on the application, the cluster analysis may be applied iteratively to further merge the groups). Each final group of representative seasonal cycles constitutes what we refer to as a *phenological characteristic regime.* Geographic maps of these regimes reveal large ocean areas that host a single regime or closely similar regimes; we refer to these regions as *phenological bioregions.* Similar techniques have been already used to determine bioregions, by clustering different parameters on the same pixel and then grouping pixels having similar ranges of the considered parameters [i.e., *Oliver and Irwin*, 2008; *Moore et al.*, 2001]. The approach proposed here is however different, in the sense that the pixel classification (and the consequent spatial distribution of the memberships) is based uniquely on the phenology of phytoplankton (i.e., on the seasonal cycle of the surface normalized chlorophyll), without introduction of any additional parameters. The phenological bioregions that we obtained are then not comparable with those obtained using other approaches.

[17] For each pixel of the CZCS and SeaWiFS climatologies, a vector containing the twelve monthly observations of normalized Chl concentration was extracted. The resulting M vectors were organized in two arrays of N x M size, one for each climatology, where N = number of months = 12 and M = number of pixels = 2519. Therefore the two periods where treated as completely independent. Each array was then clustered using an agglomerative hierarchical clustering method [*Hartigan*, 1975]. The number of clusters, n, is the only input parameter for this method. Its value was determined independently for each climatology by using a method introduced by *Ratkowsky and Lance* [1978] and later adapted to satellite ocean color data sets by *D'Ortenzio and Ribera d'Alcalà* [2009]. The clustering process ultimately produces two M-sized vectors (one for each climatology) that indicate the membership (i.e., the assigned cluster) of each satellite pixel. The center of each cluster was determined by computing the median over all rows of the initial array having the same cluster membership. Similarities among these cluster centers (i.e., representative seasonal cycles) from both climatologies were then assessed by again applying the same clustering technique. The resulting groupings ("Clusters") define our phytoplankton regimes (i.e., the shape of the curve that tracks normalized Chl over the climatological year). A global map of cluster memberships was also produced for each climatology to show the spatial distributions of the phenological bioregions during each time period.

2.3. Cluster Stability

[18] Statistical relevance of the clusters and memberships was checked using three different test algorithms [*D'Ortenzio and Ribera d'Alcalà*, 2009; *Hennig*, 2007]. The rationale was to verify whether the clustering results are reproduced

when the initial data set is slightly altered. Ideally, clustering results will be insensitive to noise-level or other small changes to the original data. Clusters found to be unstable—that is, overly sensitive to noise or small biases, for example–must be considered with caution. The method used here is based on *Hennig* [2007], whose approach has been previously employed to test the stability of satellite data classifications [*D'Ortenzio and Ribera d'Alcalà*, 2009; *Farmer et al.*, 2010]:

[19] 1. Hierarchical clustering was applied to the original data set of satellite observations, resulting in a first set of clusters (i.e., two sets of n "original clusters").

[20] 2. Three modified data sets were then generated for each climatology by 1) the *bootstrap* method, which uses the original clusters to introduce bias in the original data set, 2) the *noise* method, which randomly replaces 5 percent of the elements of the original data set with noise values, and 3) the *jittering* method, which adds or removes noise to every element of the original data set. Noise and errors for the noise and jittering methods were calculated using the covariance matrix of the original data set [*Hennig*, 2007].

[21] 3. For each modified data set, n clusters ("modification clusters") were calculated using the same algorithm that was used to compute the original clusters.

[22] 4. The Jaccard similarity coefficient was computed to quantitatively compare each original-cluster set with its three associated modification-cluster sets. Given two series of clusters (original and modification), the Jaccard coefficient is the number of points belonging to both series divided by the total number of points. (See *Hennig* [2007] for a formal demonstration.)

[23] 5. Steps 2 through 4 were repeated 100 times, and average Jaccard coefficients were computed.

[24] Following *Hennig* [2007], clusters with a mean Jaccard coefficient greater than 0.75 can be considered stable. This threshold value is only a general guideline, indicative of likely stability. Low Jaccard coefficients likely suggest erratic or incorrect classifications; in such cases, cluster identifications must be considered more tentative and interpretations must be made with greater caution.

3. Results

[25] The appropriate number of initial clusters, determined separately and independently for each of the five-year climatologies, turned out to be five in both cases: $n_{czcs} = n_{seawifs} = 5$ (Figure 1). Stability tests on the resulting ten ($n_{czcs} + n_{seawifs} = 10$) clusters produced mean Jaccard coefficients greater than the stability threshold value of 0.75 for most clusters (Table 1). The coefficients are generally higher for clusters from the 1979–1983 data set. The bootstrap and noise tests for two of the clusters for the period 1998–2002 (identified as Tropical and Subtropical South, discussed below) produced Jaccard values lower than 0.7; the Tropical noise test produced a value less than 0.6. These two clusters of the 1998–2002 period may therefore be statistically less relevant than the other clusters and should be interpreted with caution.

[26] Among the ten seasonal cycles (Figures 1a–1f), which correspond to the centers of the clusters for the two time periods, some similarities were apparent. To quantify these resemblances and facilitate interpretation, similar cycles were grouped together, again using a clustering technique. Four resulting groups (Clusters #1, #2, #3, and #4) were found to contain statistically similar members from both time periods (Figures 1a–1d). One seasonal cycle from each era—assigned to Cluster #5 (1979–1983 only; Figure 1e) and Cluster #6 (1998–2002 only; Figure 1f)—did not show statistical similarity to any other temporal cycle. For comparison, Figure 1g shows the mean seasonal cycle for SeaWiFS pixels within areas identified as belonging to Cluster #5 of the 1979–1983 period. Similarly, Figure 1h shows the mean seasonal cycle of CZCS pixels located in areas assigned to Cluster #6 of the 1998–2002 period. Membership maps showing Cluster assignments for each pixel of the 1979–1983 and 1998–2002 cliamtologies are shown in Figures 2a and 2b.

[27] Standard deviations were calculated to indicate the variability of normalized Chl for each month within the climatology-specific clusters (Figures 1a–1f) and the comparison (non-cluster) seasonal cycles (Figures 1g and 1h). The standard deviation was calculated on all pixels within a cluster for a given month regardless of pixel location.

[28] The main feature of Cluster #1 (Figure 1a) is a normalized-Chl peak in April/May, followed by a summertime low. A secondary peak in November/December is observed in only the 1979–1983 seasonal cycle. This Cluster is observed almost exclusively in the Northern Hemisphere (Figure 2) and corresponds to model number 2 of the *Longhurst* [1995, 1998] classification (*Westerlies domain: midlatitude nutrient-limited spring production peak*). An important differentiating feature of this Cluster is the sharp springtime peak. We refer to this Cluster as the *Bloom* regime.

[29] Cluster #2 (Figure 1b) is similar to model 4 of the *Longhurst* [1995, 1998] classification (*Tropics*, named here *Tropical*). In this Cluster, normalized Chl concentration varies only weakly across the seasons. Slight differences between the two periods are observed, with the 1979–1983 curve showing a minor summertime dip. This Tropical Cluster occurs predominantly in the Northern Hemisphere tropical belt (between the equator and 20°N) during both time periods (Figure 2). It's important to keep in mind that this cluster—and all others—is defined not by its geographic location but by the shape of the curve that tracks normalized Chl over the climatological year (e.g., Figure 1b). So-called Tropical cycles may well occur in nontropical locations; the key point is that the seasonal cycles in these areas are relatively flat, with little variability observed in normalized Chl over the course of the year.

[30] Clusters #3 and #4 have similar seasonal evolutions, with one shifted by about six months from the other. Cluster #3 shows a normalized-Chl peak in January/February, while Cluster #4 exhibits a maximum in August/September. These phenological Clusters correspond to Longhurst's model 3 (*Subtropical winter nutrient-limited*). Cluster #3 is observed almost exclusively in the Northern Hemisphere, and we named it *Subtropical North.* Cluster #4 is observed predominantly in the Southern Hemisphere, and we refer to it as the *Subtropical South* regime. During the 1998–2002 period, Cluster #4 is also observed in equatorial regions of the western Indian Ocean and western Atlantic. The Subtropical Clusters exhibit a pronounced to moderate seasonality (i.e., difference between annual maximum and minimum) but are

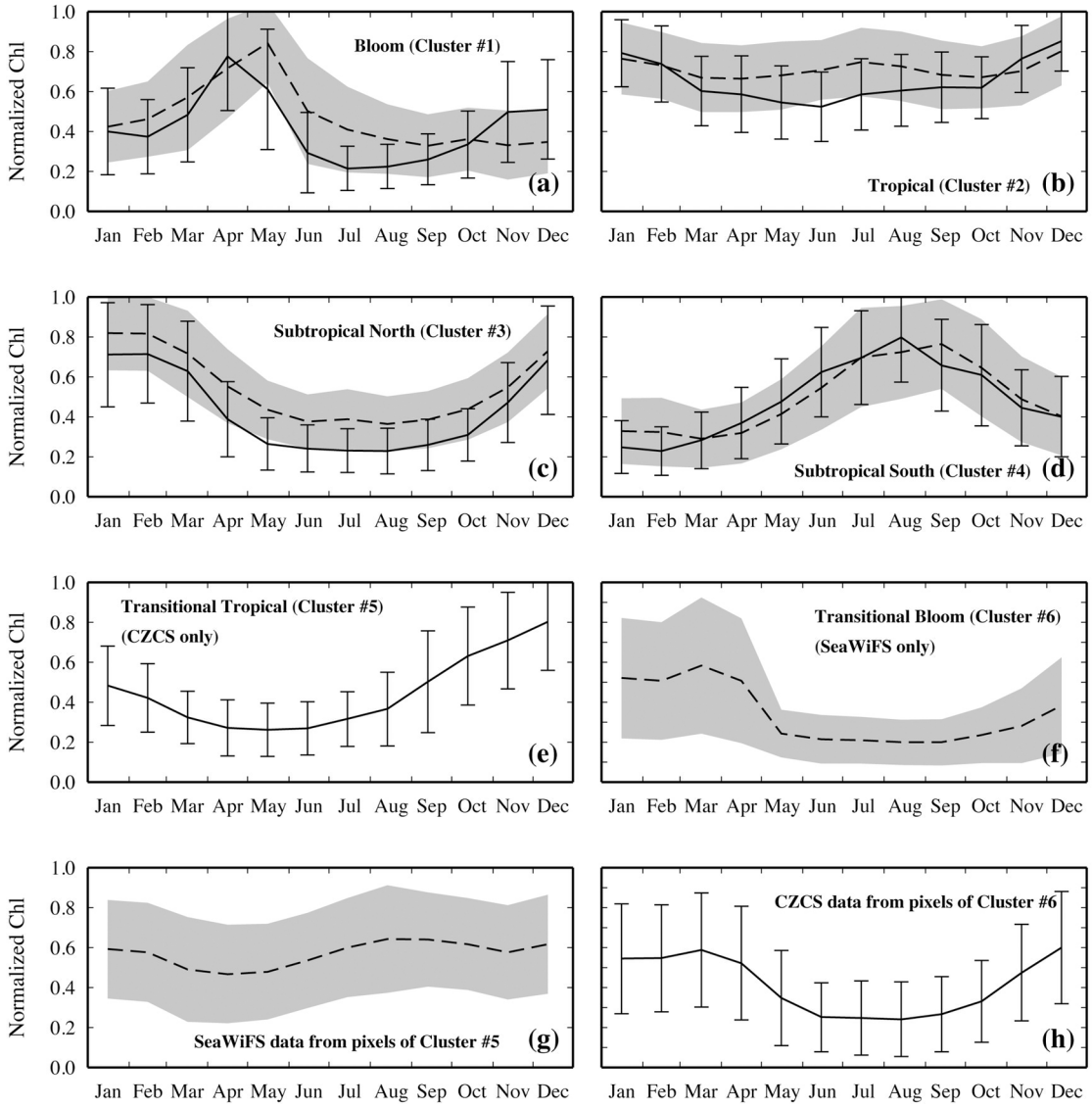

Figure 1. Centers of the ten clusters identified in the Coastal Zone Color Scanner (CZCS) and Sea-viewing Wide Field-of-view Sensor (SeaWiFS) data sets and their regime assignments. Solid lines: 1979–1983 period (CZCS); dashed lines: 1998–2002 period (SeaWiFS). Standard deviations are indicated as vertical bars for the CZCS period and as shaded areas for the SeaWiFS period. Panels a–d show the clusters of the four regimes common to both time periods. Panels e and f show the two regimes observed in only one period or the other. Panel g shows the mean seasonal cycle of SeaWiFS pixels in areas assigned to the CZCS-only Cluster #5. Panel h shows the mean seasonal cycle of CZCS pixels in areas assigned to the SeaWiFS-only Cluster #6.

differentiated from the Bloom Cluster by the timing of the peaks.

[31] The remaining two Clusters, #5 and #6, are seen during only one time period or the other. Cluster #5, observed in the 1979–1983 data only (Figure 1e), is similar to the Tropical Cluster but with a highly enhanced tail at the end of the year. This cycle shows maximum normalized Chl values in December and minima in Apr/June and is located within the equatorial belt (Figure 2a). This regime seems to be intermediate between the Tropical and Subtropical North Clusters; consequently, we refer to it as *Transitional Tropical.* Cluster #6, observed in the 1998–2002 data only (Figures 1h and 1f), appears to be a transition or intermediate regime between the Bloom and Subtropical North Clusters; we refer to it as the *Transitional Bloom* regime. A key feature of this Cluster is its relatively muted seasonality. No patterns similar to Clusters #5 and #6 are present in the Longhurst models. However, as will be further developed in the Discussion section, these two Clusters can be interpreted as subclasses of the Bloom, Tropical, and Subtropical North regimes. In this sense, they still fall within the Longhurst classification scheme, though they describe some specific conditions that lie outside the scope of Longhurst's analyses. Transitional Tropical and Transitional Bloom regimes may appear not only during times of transition from one fundamental regime to another; they may also

Table 1. Average Jaccard Coefficients (Stability Test Results) for the Climatology-Specific Clusters Obtained From the Two Ocean-Color Data Sets, 1979–1983 (CZCS) and 1998–2002 (SeaWiFS)[a]

	1979–1983					1998–2002				
	Bloom	Tropical	Subtropical North	Subtropical South	Transitional Tropical	Bloom	Tropical	Subtropical North	Subtropical South	Transitional Bloom
Bootstrap	0.95	0.88	0.91	0.93	0.99	0.79	0.65	0.82	0.66	0.88
Noise	0.99	0.95	0.96	0.98	0.99	0.82	0.56	0.72	0.63	0.89
Jitter	0.99	0.99	0.99	0.99	0.99	0.99	0.99	0.99	0.99	0.99
Average	0.98	0.94	0.95	0.97	0.99	0.86	0.73	0.84	0.76	0.92

[a]A value greater than 0.75 is indicative of cluster stability.

arise as an apparent intermediate state when multiyear averages are used to characterize regions and times of significant interannual variability.

[32] The patterns emerging for years 1998–2002 are very similar to the patterns characterizing the full SeaWiFS record (1998–2010; Figures 3 and 4). Over the 1998–2010 period, the Transitional Bloom regime displays a higher seasonality (difference between minima and maxima in the normalized chlorophyll) and a larger geographical extension than in the 1998–2002 subset. A one-month shift is present in the occurrence of the maximum in the Bloom regime, which displays a smaller geographically extension at the expense of the Transitional Bloom. The Transitional Bloom is more significant than the Bloom and the Subtropical North, which

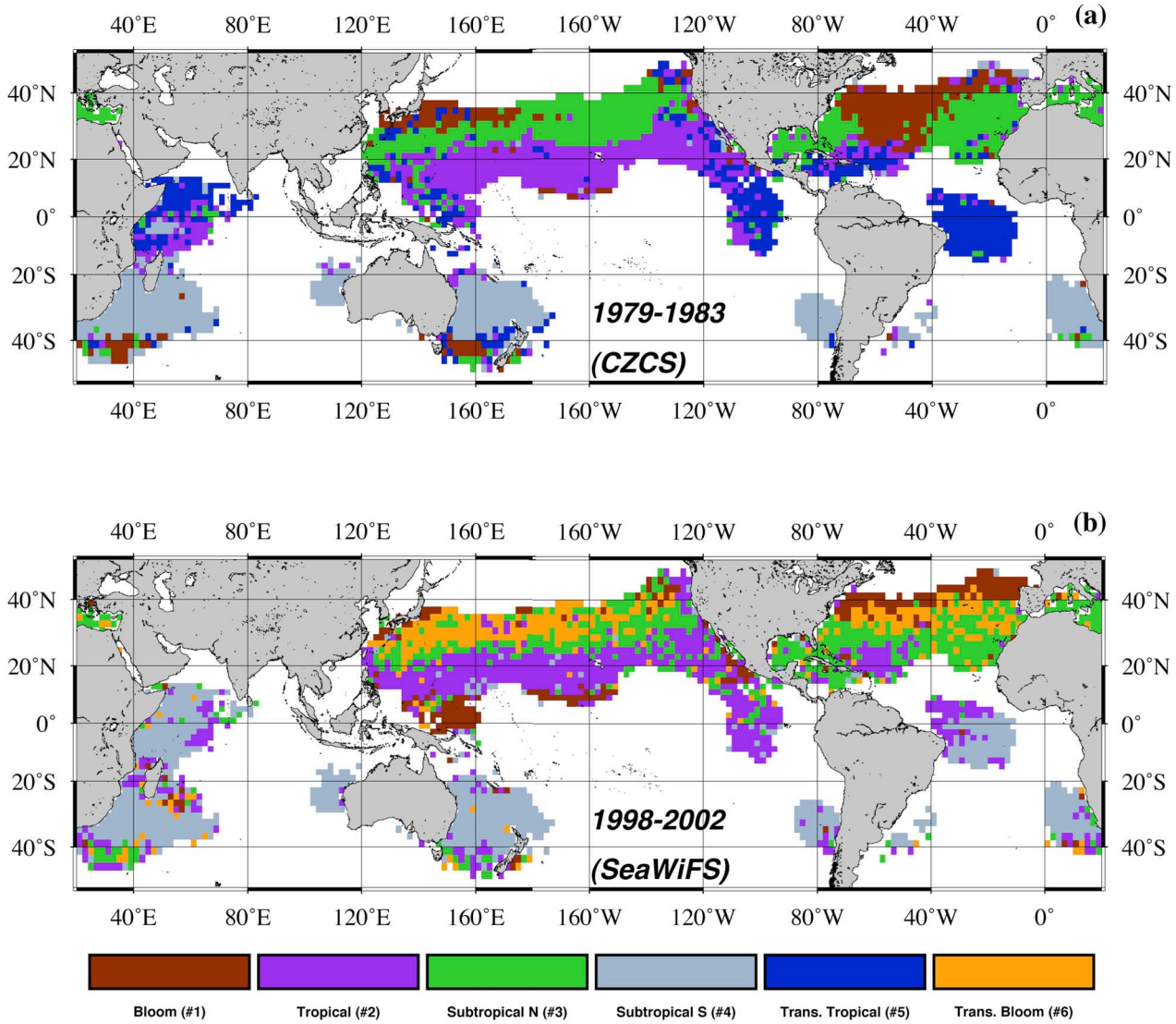

Figure 2. Cluster-derived maps of phenological regimes for (a) the CZCS period (1979–1983) and (b) the SeaWiFS period (1998–2002).

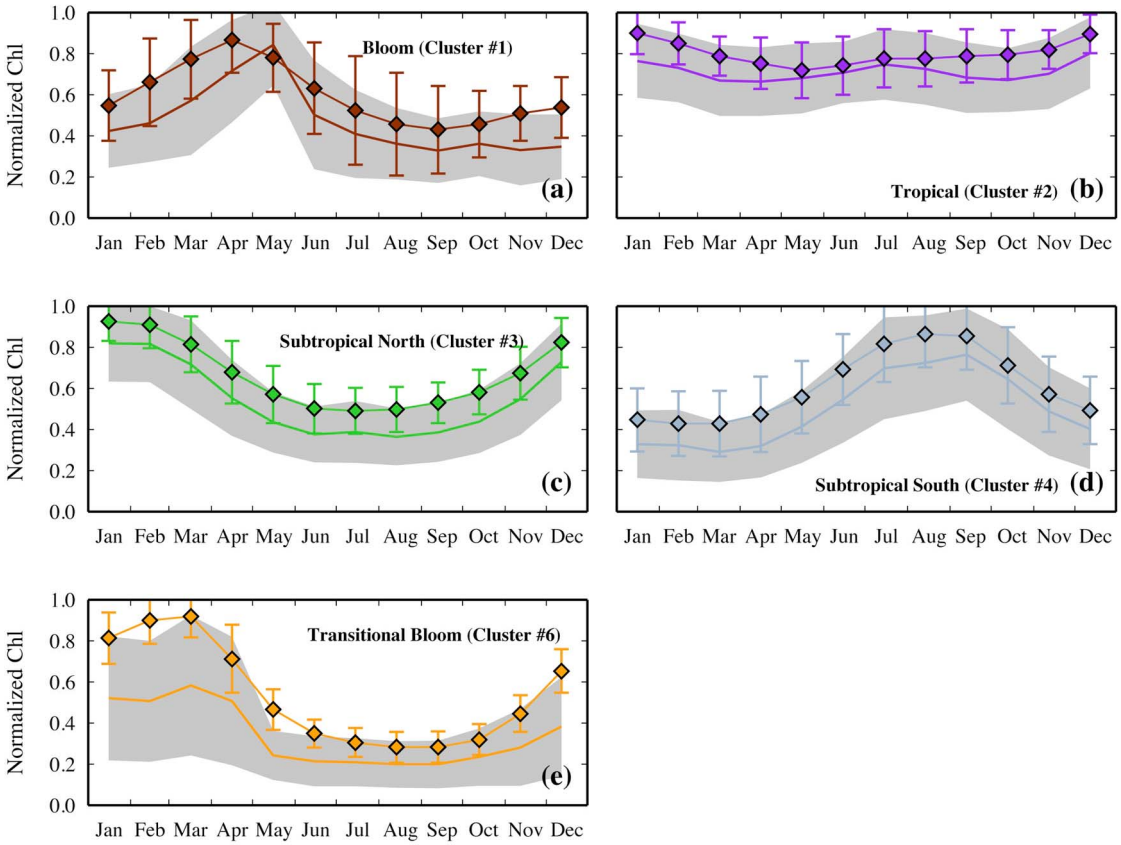

Figure 3. Centers of the clusters identified in the complete SeaWiFS data sets (1998–2010) and in the reprocessed SeaWiFS data sets (1998–2002). Lines: reprocessed data sets (1998–2002, as in Figure 1); diamonds: full SeaWiFS record (1998–2010). Standard deviations are indicated as vertical bars for the full SeaWiFS record and as shaded areas for the reprocessed SeaWiFS period.

is a further clue for it being a combination of the two regimes. Overall, although some slight differences appear between the clusters obtained from the standard 1998–2010 and the reprocessed 1998–2002 SeaWiFS data, both cluster-analysis highlights the same changes compared with the 1979–1983 CZCS time period.

[33] We also performed two cluster analyses separately for El Niño and La Niña years, using the 1998–2010 SeaWiFS data set (Figure 7). The years 1998, 2003, 2005, 2007, and 2010 were assigned to El Niño conditions and 1999, 2000, 2001, 2008, 2009 to La Niña [*Radenac et al.*, 2012]. A first goal of these two analyses is to determine to what extent our averaging over 5 years could mask significant patterns determined by these large-scale oceanic processes. Four of the seasonal cycles obtained on the 1998–2002 clustering are confirmed also in the clustering of the El Niño and La Niña years. The Transitional Bloom regime appears only during La Niña years. A new Cluster is sporadically observed during the El Niño years (black pixels in Figure 7). It does not show any meaningful spatial patterns, and likely results from the grouping of pixels that could not fit the dominant patterns (i.e., it is a statistical artifact). It is not further considered. North of 20°N, most of the pixels are classified as Subtropical North or Bloom regime during El Niño years, with a clear North-South pattern. During La Niña years, most of the pixels (82%) changed their membership in Transitional Bloom. Very few changes between El Niño and La Niña years are observed elsewhere (only 15% of pixels south of 20°N change membership).

[34] Overall, the comparison between the 1998–2002 and 1998–2010 SeaWiFS data set confirms the persistence of the main seasonal cycles of normalized chlorophyll concentration, when obtained either from the 1998–2002 climatology (Figures 1 and 3) or from the 1998–2010 climatology (Figure 4) or from separate groupings of El Niño and La Niña years (Figure 7). The spatial distributions of the Clusters are, however, different (Figures 4 and 7).

4. Discussion

4.1. Oceanographic Relevance of Cluster-Based Phytoplankton Phenology

[35] As discussed below, several lines of evidence indicate that the seasonal-cycle clusters are not merely statistical entities but are in fact oceanographically relevant. Four regime clusters were identified in ocean-color data from both the periods 1979–1983 and 1998–2002: Bloom, Tropical, Subtropical North, and Subtropical South. Because the cluster identifications were performed independently on the CZCS and SeaWiFS data archives, the four clusters likely represent real environmental patterns. In addition, these four persistent clusters match previously identified patterns of

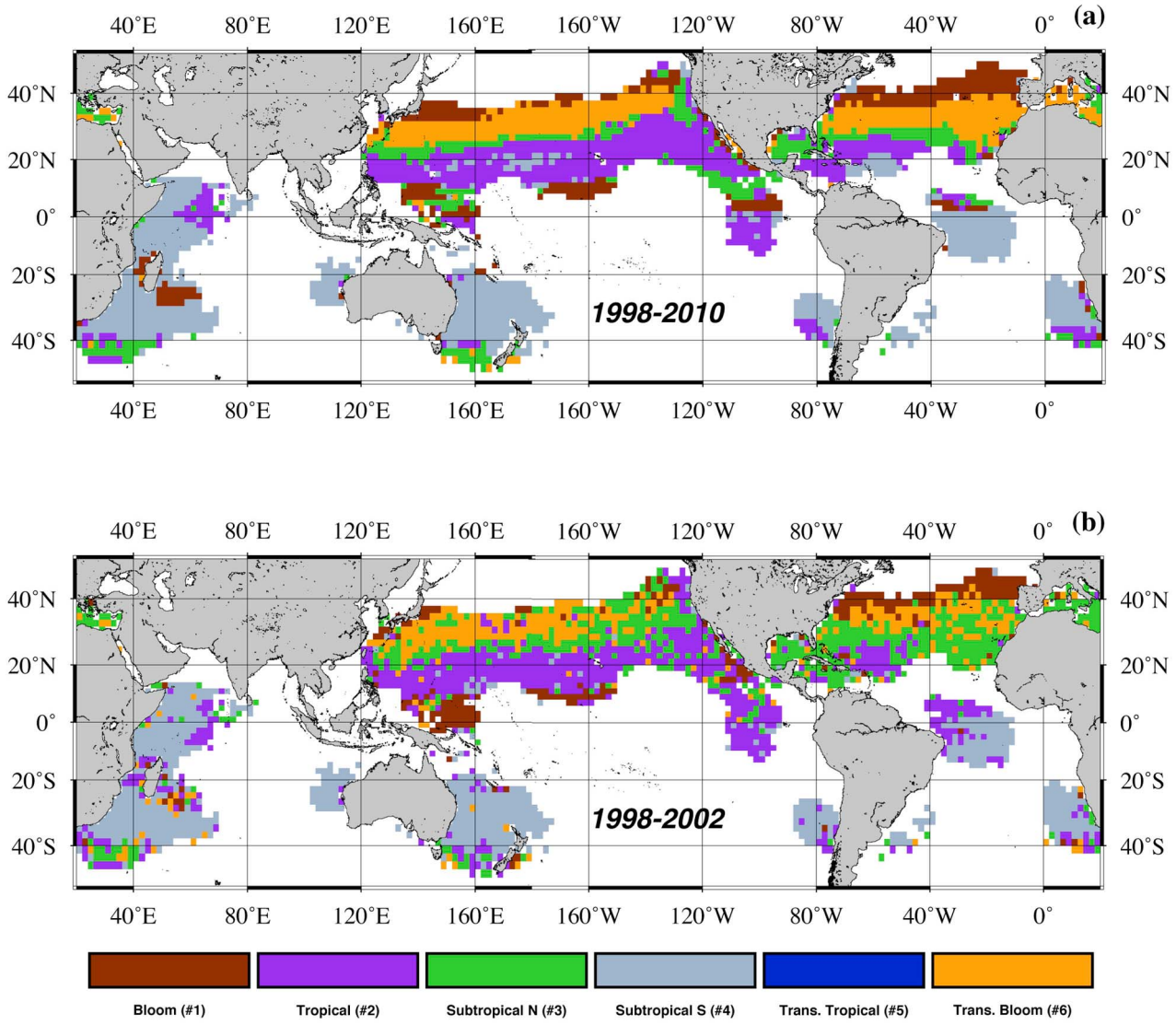

Figure 4. Cluster-derived maps of phenological regimes for (a) the complete SeaWiFS data set (1998–2010) and (b) the reprocessed *Antoine et al.* [2005] data set (1998–2002).

phytoplankton phenology [*Longhurst*, 1998; *Riley*, 1946; *Yoder et al.*, 1993]: Bloom, Tropical, and Subtropical (the Subtropical North and Subtropical South clusters can be considered subsets of the same Subtropical model/regime; they are simply time-shifted according to hemisphere).

[36] Assessments of oceanographic consistency must also include evaluation of the spatial patterns that arise from the cluster analyses. The membership maps (Figure 2) show that pixels belonging to the same cluster are usually contiguous. This spatial coherence is an indication that the method captures real biogeographical features of oceanic phytoplankton. In addition, most pixels were automatically assigned to clusters of the appropriate hemisphere. The few exceptions are discussed below.

[37] No predefined shapes were imposed on the cluster centers (seasonal cycles). These results, along with the statistical stability tests (Table 1), demonstrate the robustness of the adopted cluster analysis. Patterns consistent with oceanographic observations and expectations were obtained without the input of any a priori hypothesis.

4.2. Phytoplankton Phenology in the Periods 1979–1983 and 1998–2002

[38] For ~35% of the areas analyzed, cluster membership did not change from 1979 to 1983 to 1998–2002 (dark gray areas in Figure 5). In the remaining ~65% of the pixels, the most conspicuous phenological changes were the emergence of the Transitional Bloom regime (blue and green areas, Figure 5) and the disappearance of the Transitional Tropical regime (purple and pink areas, Figure 5). More precisely, 13.5% of the 1979–1983 pixels changed their membership in Transitional Bloom, and 19% of the 1979–1983 changed their membership from Transitional Tropical to another regime. To further explore these changes of cluster membership, we looked to characterizations of upper-ocean stratification, reports of widespread decadal-scale ecosystem-

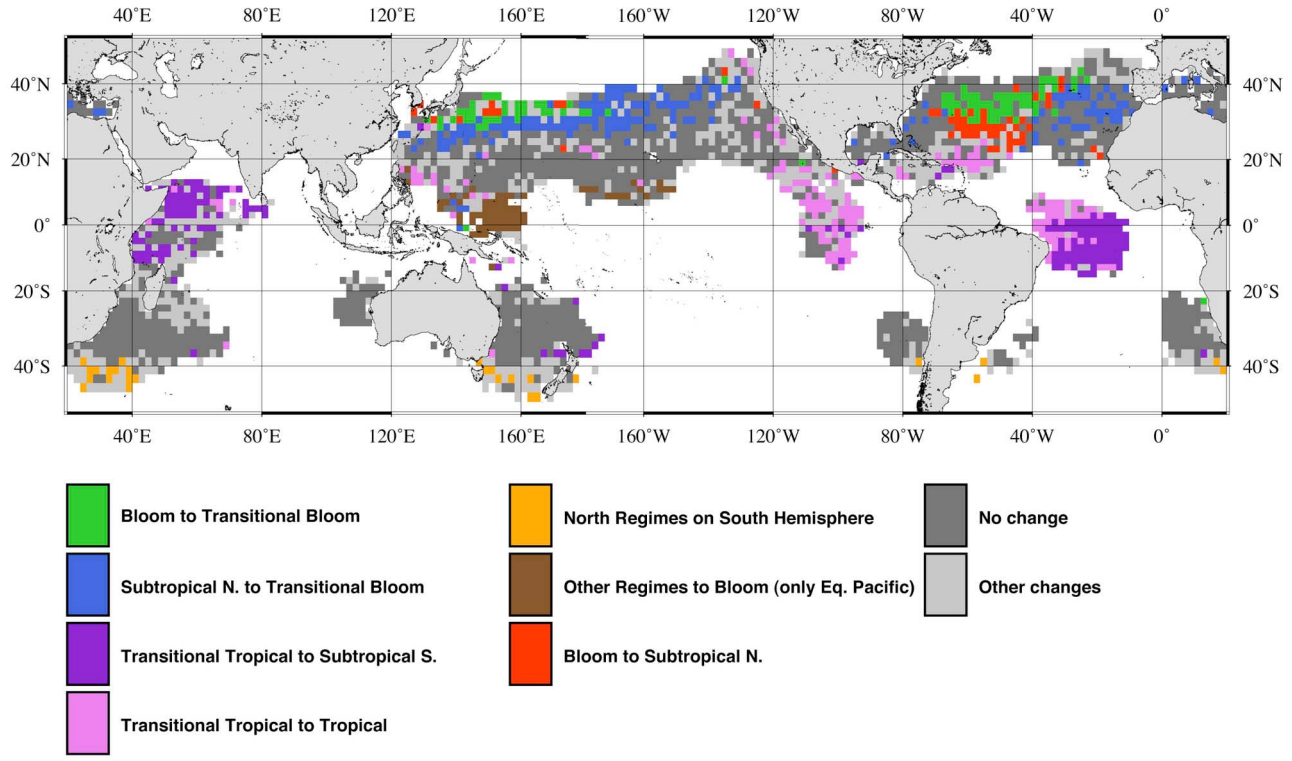

Figure 5. Changes in cluster membership between the CZCS (1979–1983) and SeaWiFS (1998–2002) time periods.

related change (e.g., Chl concentrations), and changes in large-scale climate indices and their oceanic signatures. To map mixed-layer behavior specifically, changes in the average annual maximum mixed layer depth (MLD; Figure 6a) and the timing of the annual maximum (Figure 6b), we relied on Simple Ocean Data Assimilation (SODA) model output [*Carton and Giese*, 2008]. The MLD is determined using a temperature criterion, as being the depth where the temperature is 0.2°C different from the temperature at 10 m [*de Boyer Montégut et al.*, 2004].

[39] Dissecting the phenological signal is extremely complicated. Phytoplankton temporal evolution in a given location results from both "bottom-up" processes linked to physical environmental conditions and "top-down" processes linked to more biologically mediated interactions [*Ji et al.*, 2010]. In this work, we focus largely on upper-ocean stratification, for which data are more readily available, as a reasonable starting point for exploring the observed 20-year shifts in phytoplankton phenology.

4.2.1. Emergence of the Transitional Bloom Regime

[40] Emergence of the Transitional Bloom regime during the 1998–2002 SeaWiFS years is observed in the 20°–40°N latitudinal belt of both the Atlantic and Pacific Oceans (green and blue regions in Figure 5). This "new" regime replaces much of the Bloom and Subtropical North regimes of the 1979–1983 CZCS years: nearly a third of each of these original regimes had converted to Transitional Bloom (Table 2). We have also shown that this replacement is even more important if the whole SeaWiFS series (1998–2010) is considered, but also that it is dominant during La Niña years.

[41] One area that changed from Bloom to Transitional Bloom (green regions in Figure 5) is the western subtropical North Atlantic. Phenologically (Figures 1a and 1f), this change can be seen in both the seasonality (i.e., difference between annual maximum and minimum) of the normalized surface Chl and the timing of the peak. Seasonality during the 1998–2002 period (Figure 1f) is relatively muted, and the time of peak normalized Chl is shifted earlier by two months (from May to March). SODA mixed layer depths show a general shoaling of the annual maximum depth over that same time period (Figure 6a); no change in the timing of the maximum was observed (Figure 6b). Chlorophyll concentrations in this region generally diminished between the 1979–1983 years and the 1998–2002 years [*Antoine et al.*, 2005; *Martinez et al.*, 2009]. Both these lines of evidence (decreased mixing and generally lower Chl concentrations), as well as the shift to a more muted seasonality, are consistent with a presumed reduction in nutrient flux to the upper layer, related to enhanced upper-ocean stratification [as proposed by *Behrenfeld et al.*, 2006; *Follows and Dutkiewicz*, 2001].

[42] For subpolar North Atlantic regions, the timing of the chlorophyll peak, variability of mixed layer depth [*Henson et al.*, 2009], and abundance of zooplankton [*Beaugrand et al.*, 2000] have all been correlated with the North Atlantic Ocean (NAO) index [*Hurrell*, 1995]. Such NAO correlations are less evident, however, for the subtropical areas (25°N–40°N) [*Carton et al.*, 2008; *Henson et al.*, 2009] where we observed the change from Bloom to Transitional Bloom. A more relevant index for this region is the Atlantic Multidecadal Oscillation (AMO) index, which tracks the

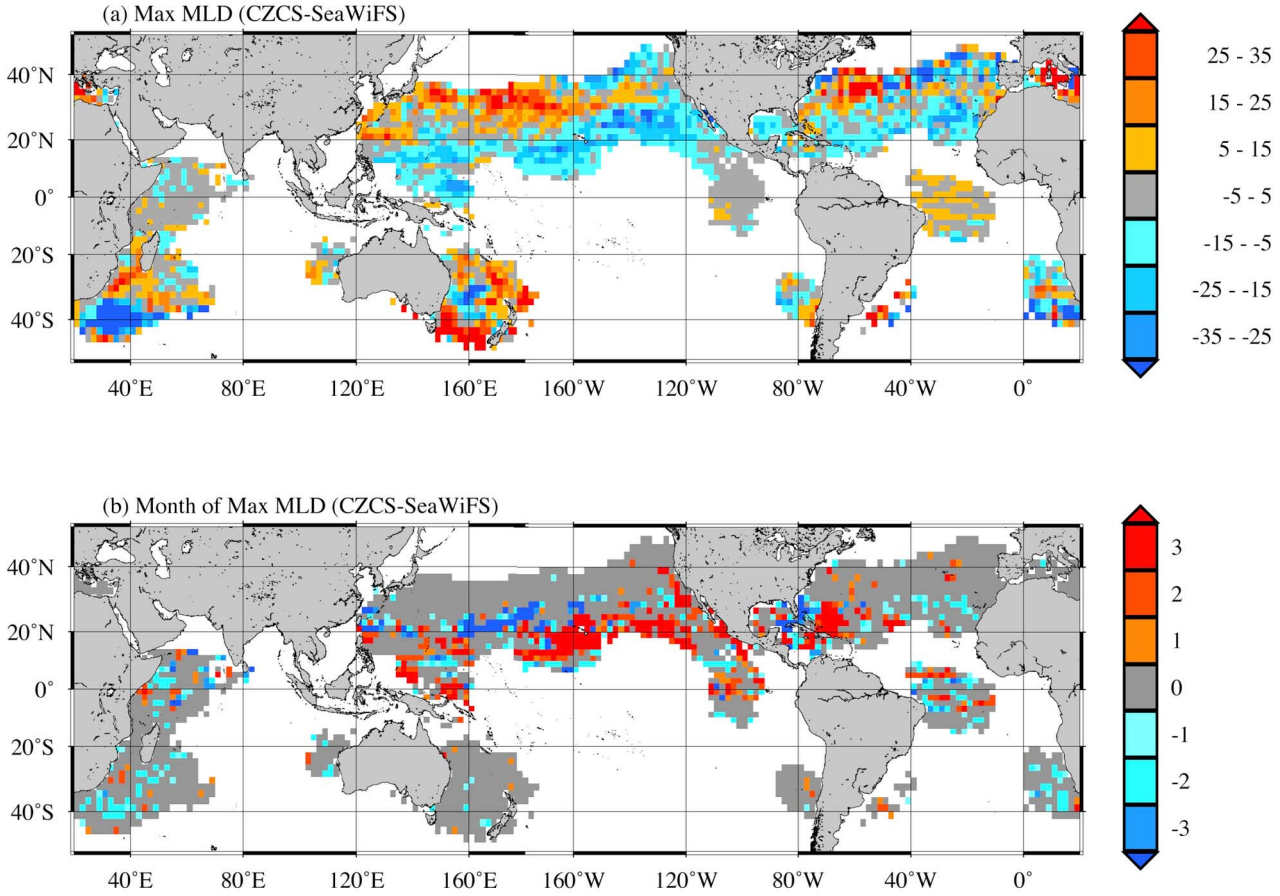

Figure 6. (a) Differences in annual maximum mixed layer depth (MLD) between the two time periods: CZCS minus SeaWiFS. Positive values (warm colors) indicate deeper maximum MLDs during CZCS times; negative values (cool colors) indicate deeper maximum MLDs during the SeaWiFS period. (b) Differences in timing of the annual maximum of MLD (in months). For pixels with positive values (warm colors), the MLD annual maximum occurred later in the year during the CZCS period than during the SeaWiFS period.

long-term detrended mean of North Atlantic Ocean sea surface temperature (SST), revealing cycles of about 65–80 years duration [*Enfield et al.*, 2001]. This index has been found to correlate with chlorophyll–SST long-term variability in the North Atlantic [*Martinez et al.*, 2009]. The AMO index shifted from negative (cool phase) during the 1979–1983 CZCS years to positive (warm phase) during 1998–2002 SeaWiFS years. This overall increase of North Atlantic SST and likely consequent increase in upper-layer stratification is also consistent with the results of our mixed-layer and phenological analyses in the Western sub tropical Atlantic—i.e., generally shoaling mixed layer annual maximum depths (red regions in Figure 6) and generally muted normalized-Chl seasonality (green pixels in Figure 5).

Table 2. Changes in Regime Assignments Between the Periods 1979–1983 (CZCS) and 1998–2002 (SeaWiFS)[a]

1979–1983		1998–2002				
Regimes and Seasonal Cycles	Total Number of Pixels for the CZCS Period	**Bloom**	**Tropical**	**Subtropical North**	**Subtropical South**	Transitional Bloom
Bloom	288	*28%*	13%	23%	6%	**31%**
Tropical	610	11%	***57%***	17%	13%	3%
Subtropical North	602	5%	10%	***52%***	2%	30%
Subtropical South	524	4%	12%	3%	*77%*	4%
Transitional Tropical North Hemisphere	274	7%	**42%**	22%	20%	9%
Transitional Tropical South Hemisphere	221	5%	28%	5%	**60%**	3%

[a]The leftmost columns show the initial apportionment of regime memberships among pixels for the years 1979–1983. For each of these regimes (rows), the percentages indicate the pixel transitions that occurred over the next two decades. The regimes set in bold type were observed during both time periods. For these four persistent regimes, the numbers in italics (i.e., on the diagonal) indicate the percentage of pixels that registered no change of cluster membership. The percentages set in bold type indicate the single most common fate of a given regime's pixels.

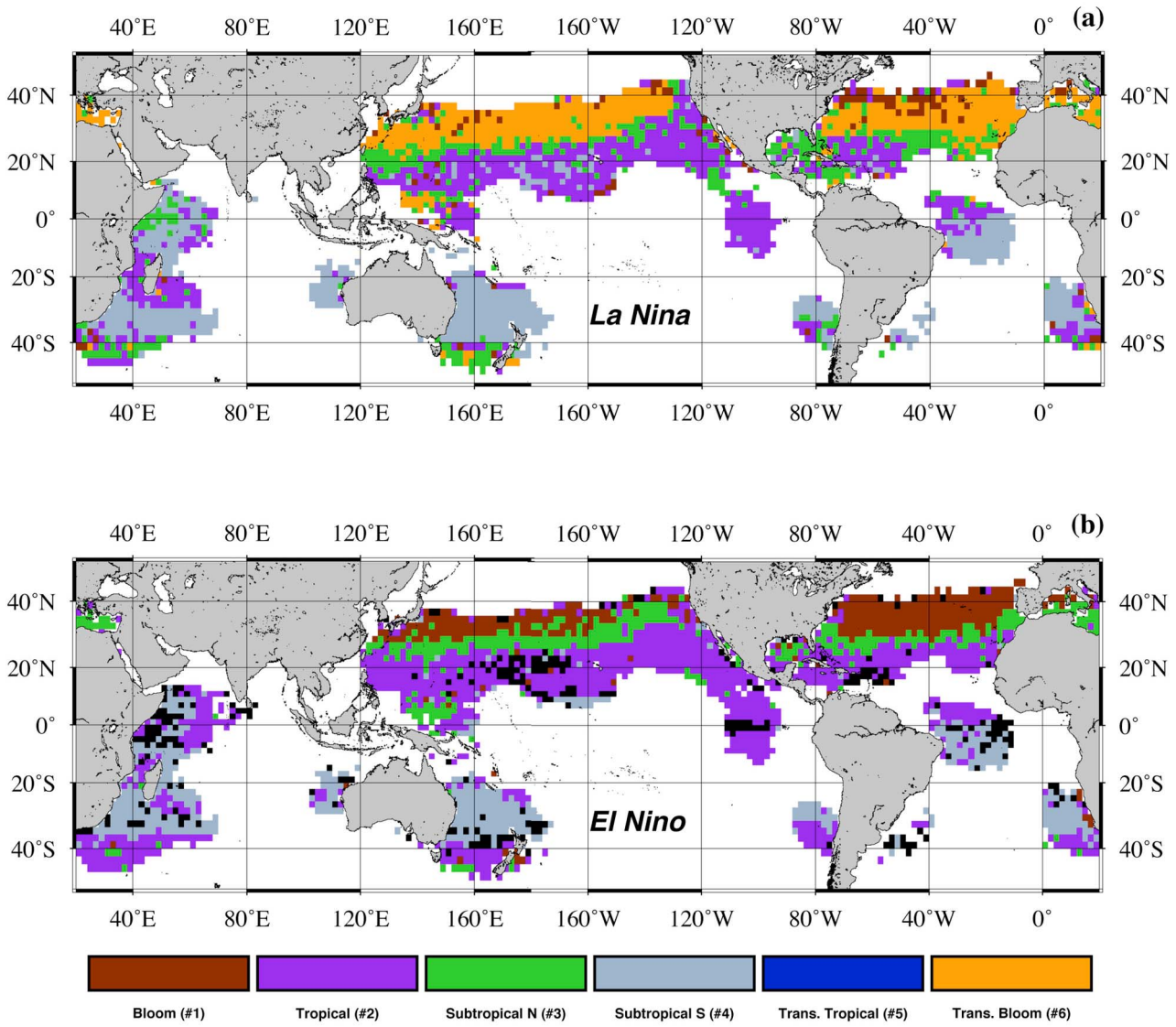

Figure 7. Cluster-derived maps of phenological regimes for (a) La Niña and (b) for El Niño years over the 1998–2010 SeaWiFS time period.

[43] In other areas of the subtropical North Atlantic, we observe shifts from Bloom to Subtropical North (red regions in Figure 5) and, to a lesser extent, from Subtropical North to Transitional Bloom (blue regions in Figure 5). Overall, these changes describe a general dampening of the differences between seasonal minima and maxima and a spreading of the 'growth' season over one or two additional months (Figure 1). Other analyses document a decrease in upper-ocean chlorophyll content in these regions, as observed comparing the trends for two disconnected climatologies of the 1979–1983 and 1998–2002 years [*Antoine et al.*, 2005; *Martinez et al.*, 2009] but also more continuously over the period 1998–2006 [*Behrenfeld et al.*, 2006]. The phenological change of the whole subtropical North Atlantic Ocean could be linked to enhanced stratification, which may in turn be related to the SST variability indicated by the AMO index (i.e., enhanced stratification during AMO warm, positive-index phases).

[44] Transitional Bloom emergence is also observed in the Kuroshio area, replacing earlier Bloom conditions (western North Pacific; green pixels in Figure 5). Here, chlorophyll concentrations decreased between 1979–1983 and 1998–2002 [*Martinez et al.*, 2009] and mixed layer depth annual maxima shoaled (Figure 6a), similar to the pattern observed in the North Atlantic. No change was observed in the timing of peak normalized chlorophyll (Figures 1a and 1f) or annual maximum depth of mixing (Figure 6b).

[45] Widespread emergence of the Transitional Bloom regime occurred in the North Pacific along the longitudinal belt of 20°–30°N, replacing the Subtropical North regime observed in the period 1979–1983 CZCS (blue regions in Figure 5). This change implies a delay of about one month in the phytoplankton annual maximum (from February to March) and a smoothed seasonality (Figures 1c and 1f). SODA MLDs (Figure 6) indicate a shoaling of the maximum mixed layer depth and no change in the timing of the

maximum. A general decrease of surface chlorophyll concentrations was observed over this time period [*Antoine et al.*, 2005; *Martinez et al.*, 2009].

[46] The region of this major phenological change is located approximately along the Pacific Transition Zone Chlorophyll Front (TZCF) [*Polovina et al.*, 2001], a dynamic, seasonally migrating, basin-wide front that divides the high-chlorophyll subarctic gyre from the low-chlorophyll subtropical gyre. Strong chlorophyll seasonality is observed to the north of the front and weak seasonality to the south [*Longhurst*, 1995]. During El Niño winters, the front migrates especially far southward, to move northward during La Niña periods [*Bograd et al.*, 2004]. During the 1979–1983 CZCS years (which included a strong El Niño event), the TZCF exhibited its greatest observed range of migration and southward extent [*Bograd et al.*, 2004]. This frontal behavior is consistent with the phenological conditions we detected–i.e., the presence of the Subtropical North regime (moderate seasonality) in the longitudinal belt of 20°–30°N. The subsequent emergence of the Transitional Bloom regime (relatively muted seasonality) is similarly consistent with the observed shrinkage and more northerly position of the TZCF during the 1998–2002 SeaWiFS years, which comprises at least three La Niña events [*Radenac et al.*, 2012]. This effect of the El Niño/La Niña on the TZCF, and, in turn, on the phytoplankton phenology of the subtropical North Pacific, is confirmed by the separate analysis of the El Niño and La Niña years on the 1998–2010 data set (Figure 7).

[47] The TZCF position is correlated with the strength of the Aleutian Low [*Bograd et al.*, 2004; *Peterson and Schwing*, 2003], which is in turn related to the Pacific Decadal Oscillation [*Mantua and Hare*, 2002; *Mantua et al.*, 1997]. The PDO index is widely used to characterize North Pacific atmosphere–ocean–ecosystem variability. Twentieth-century events typically lasted 20 to 30 years [*Mantua and Hare*, 2002; *Mantua et al.*, 1997] and appear to be driven in equals parts, at decadal scale, by the variability of the Aleutian Low, the ENSO and the zonal advection anomalies of the Kuroshio-Oyashio extension [*Schneider and Cornuelle*, 2005]. In 1977, the PDO experienced a major polarity shift and entered a positive ("warm") phase, typically characterized by anomalously warm SSTs along the coasts of North and South America, anomalously cool SSTs in the central North Pacific, enhanced North Pacific counterclockwise wind stress [*Mantua and Hare*, 2002], and a deepened mixed layer north of 25°N [*Carton et al.*, 2008; *Di Lorenzo et al.*, 2008]. Subsequent years (the CZCS years) saw a stronger Aleutian Low, a southward shift of westerly winds, and the aforementioned southerly TZCF excursion [*Bograd et al.*, 2004; *Peterson and Schwing*, 2003]. Our detection of the Subtropical North regime (moderate seasonality) in the 20°N–30°N belt could well be an element induced by the PDO positive phase.

[48] During the 1998–2002 SeaWiFS period, the PDO index was negative, but atmospheric and SST patterns were different from classical cool-phase conditions [*Bond et al.*, 2003]. There are some indications that the North Pacific Gyre Oscillation (NPGO)—i.e., changes in gyre circulation intensity—may better explain large-scale ecosystem variability of 1998–2002 years than does the PDO [*Di Lorenzo et al.*, 2008]. The NPGO index, which was strongly positive during the 1998–2002 SeaWiFS years, has been promoted as a primary indicator of upwelling strength and associated biogeochemical change (e.g., nutrient fluxes and Chl concentrations) off the California coast [*Di Lorenzo et al.*, 2008]. Large-scale effects on ecosystems of the open Pacific basin remain somewhat speculative, and the role of the NPGO in forcing the phenological changes we observed is at present unclear. We can hypothesize that if present suspicions are confirmed (i.e., if the NPGO does turn out to be a strong indicator of large-scale variability), then it may, through its influence on Aleutian Low and TZCF variability, ultimately be found to drive the phenology of the subtropical North Pacific's surface chlorophyll.

[49] Overall, considering the main features of Transition Bloom regime (i.e., longer and flatter 'growth' season, reduced difference between minima and maxima, highstandard deviation), we interpret the widespread emergence of Transitional Bloom during the l998–2002 period (Figures 2b, 3, 4, and 5) as the weakening of a strong latitudinal seasonality gradient observed during the 1979–1983 years. The Transitional Bloom, which replaces geographically the Bloom and Subtropical bioregions, reflects then a much higher zonal variability in the phenological regimes of the Northern Hemisphere. Phytoplankton in affected areas lost synchrony and fragmented the pronounced seasonality characterizing the previous period. This regime shift would be consistent with an overall decrease in the upward flux of nutrients due to stronger upper-ocean stratification (i.e., shallower MLDs; Figure 6a), likely coupled with a larger spatial and interannual variability in the dynamics of the mixed layer. It would also be consistent with changes in other processes, such as a stronger coupling between producers and grazers (more akin to a classical Tropical regime), but data are not available to assess the relative contributions of the many potential contributing factors, particularly those that involve trophic interactions. If we confine our attention to first-order bottom-up controls on phytoplankton phenology, we can say that the appearance of the Transitional Bloom regime during the 1998–2002 period indicates a general smoothing of the normalized-chlorophyll seasonality in the Northern Hemisphere if averaged at large scales, due in large part to a change mixed layer dynamics [*Carton et al.*, 2008] and a consequent increase of variability in the phase of the seasonal cycle. This mechanism to explain the appearance of Transitional Bloom is partially confirmed by our analysis of the El Niño/La Niña years. We observe Transitional Bloom only during La Niña years. During these years, the variability of atmospheric forcing in the Northern Hemisphere increases respect to the mean state [i.e., *Li and Lau*, 2012], likely inducing the modifications of the mixed layer dynamic, which are supposed to determine the appearance of the Transitional Bloom. It is worth noting, however, that the *Radenac et al.* [2012] classification we used to group La Niña/El Niño years is different from others [i.e., *McPhaden et al.*, 2011], which makes the explanation of the link La Niña-Transitional Bloom very preliminary and worthy for further analysis.

4.2.2. Disappearance of the Transitional Tropical Regime

[50] During the 1979–1983 years, the Transitional Tropical regime occupied most of the tropical ocean belt (Figure 2). By the 1998–2002 years, though, this regime had been replaced by others (Table 2). In the Indian Ocean along the east coast of central Africa, Transitional Tropical shifted

to Subtropical South (purple pixels in Figure 5), and in the western equatorial Atlantic and the eastern tropical and subtropical Pacific, it shifted to Tropical (Table 2; pink pixels in Figure 5). In other words, conditions had apparently become generally less tropical (i.e., with heightened seasonality) in the Indian Ocean and generally more tropical (more muted seasonality) in the western equatorial Atlantic and eastern and subtropical Pacific.

[51] In the Indian Ocean, monsoonal dynamics typically induce a first bloom in summer and a secondary weaker bloom in late fall–winter, with little interannual variability [*Marra and Barber*, 2005; *Yoder et al.*, 1993]. This pattern of a strong summertime bloom is more similar to our Subtropical South regime (observed during the 1998–2002 SeaWiFS years; Figure 2b) than to Transitional Tropical (obtained during the 1979–1983 CZCS period; Figure 2a), which exhibits no summertime bloom. This apparent shift from winter bloom (during 1979–1983) to summer bloom (in the 1998–2002) could perhaps be ascribed to a change in the relative intensity of the summer and fall monsoons which in turn might imply interannual variability of the physical forcing [*Longhurst*, 1998; *Marra and Barber*, 2005]. However, SODA-derived mixed layer characteristics (i.e., the magnitude and timing of annual maximum depths) during the two periods are relatively constant (Figure 6), which would seem to exclude significant impacts from changes in mixed layer dynamics. An alternative explanation of the anomalous winter-bloom cluster obtained for the 1979–1983 CZCS period might be artifactual bias due to extensive summertime cloud cover [*Banse and McClain*, 1986; *Brock and McClain*, 1992; *Brock et al.*, 1992]. We are unable to attribute the apparent shift in the Indian Ocean to either real phenological change or coverage-related artifact.

[52] Similarly, in the western equatorial Atlantic the 1979–1983 CZCS Transitional Tropical regime could be considered atypical or perhaps even artifactual. In this region, summertime chlorophyll increase is driven by seasonal intensification of the trade winds [*Grodsky et al.*, 2008; *Li and Philander*, 1997; *Monger et al.*, 1997] and is modulated by high precipitation and river runoff in the westernmost area [*Dessier and Donguy*, 1994]. Our observed Tropical patterns of the 1998–2002 SeaWiFS years agree with this scenario [e.g., *Pérez et al.*, 2005]. The Transitional Tropical regime observed in the period 1979–1983, on the other hand, with its larger wintertime biomass (normalized chlorophyll) accumulation (Figure 1e), would be considered unusual for this region. The signal observed in the 1979–1983 CZCS observations was ascribed by *Deuser et al.* [1988] to river runoff; such runoff could potentially confound the cluster analysis of the reprocessed CZCS signal.

[53] The third region where we observed disappearance of the Transitional Tropical regime is in the Eastern Tropical Pacific (between 10°N and 10°S and between 90°W and 120°W). Here, the Tropical regime had become prominent during 1998–2002 (Figure 5, pink pixels). Phytoplankton seasonality in this region is characterized by a winter maximum driven primarily by nutrients advected in from the Equatorial upwelling region and the Peru current by the South Equatorial Current and from the equatorial front and the 10°N thermocline ridge by the North Equatorial Counter Current [*Pennington et al.*, 2006]. Overall, the region is strongly influenced by large-scale El Niño and La Niña interannual variability, the strength of which is tracked by the Multivariate ENSO Index (MEI) [*Wolter and Timlin*, 2011]. Typical event duration is 6–18 months [*Wang and Fiedler*, 2006]. During El Niño years (MEI positive), a deeper pycnocline in the eastern equatorial Pacific results in a diminished supply of nutrients to surface waters [*Pennington et al.*, 2006]. A general smoothing of the winter phytoplankton maximum has been observed during these positive phases [*Feldman et al.*, 1984; *Strutton et al.*, 2008]. For La Niña years (MEI negative), the sources of variability in phytoplankton seasonality are less well understood. Recent findings [*Behrenfeld et al.*, 2001] indicate that during La Niña years biomass generally increases across the whole equatorial Pacific, though this effect seems less pronounced in the east [*Strutton et al.*, 2008]. It is noteworthy, moreover, that the statistically relevance of the Tropical regime for the 1998–2002 period is low. The observed shift between the Transitional Tropical to Tropical in the Eastern Tropical Pacific could be then an artifact of the clustering method.

4.2.3. Other Regime Shifts and Transitions

[54] Other changes of more limited spatial extent were also detected in the phenological patterns between the 1979–1983 and the 1998–2002 years. The western tropical North Atlantic shifted from Bloom to Subtropical North (red pixels in Figure 5), consistent with a general shoaling of MLD maxima as previously discussed. The transitions from Tropical or Subtropical North to Bloom (brown pixels in Figure 5) on the western side of the Pacific equatorial belt is likely driven by the two strong La Niña events that occurred near the turn of the century. The 1998–1999 event is documented to have increased seasonality of surface chlorophyll in the region [*Radenac et al.*, 2012], which would be consistent with our observed emergence of the Bloom regime.

[55] In the 1998–2002 period, clusters typical of the Northern Hemisphere were assigned to a few areas of the Southern Hemisphere poleward of 40°S (e.g., the Tasman Sea and the southern edge of the Algulhas Current; gold pixels in Figure 5). These cycles exhibit a 6-month lag with the seasonal cycle of irradiance–i.e., the normalized-chlorophyll peak is offset from the maximum irradiance by half a year. In these areas, intense mesoscale activity is often observed [*Tilburg et al.*, 2002; *Weeks and Shillington*, 1994]. Such processes may decouple phytoplankton growth events from the annual illumination cycle.

[56] The transitional clusters (i.e., Transitional Tropical and Transitional Bloom regimes) represent important phenological states of oceanic phytoplankton. The notion that these clusters represent change from one regime to another is evident when mean seasonal cycles of the 1998–2002 period are calculated for pixels that during the years 1979–1983 were identified as Transitional Tropical (Figure 1e). The resulting cycle (Figure 1g) is clearly different from its predecessor. It appears more similar to the Tropical cycle (Figure 1b), which is a reasonable result for the latitudinal belt in question (Figure 2a, blue pixels; Figure 5, pink pixels). When mean seasonal cycles for the years 1979–1983 are calculated on pixels identified in the 1998–2002 years as Transitional Bloom (Figure 1f), the resulting pattern (Figure 1h) appears very similar to its successor. This similarity (persistence) supports our hypothesis that the Transitional Bloom regime, more than representing an intermediate state between the Bloom and Subtropical North, arises from

the coexistence of the two regimes in the same year and from the alternation over the years. The use of multiyear averages merged the two regimes in one unique cluster, which display then a higher variance than the others.

[57] Properly speaking, Transitional Bloom is not a new regime, but the superposition of two well-identified regimes, modulated by the interannual variability. However, its appearance/disappearance occurs during La Niña/El Niño years (Figure 7), and it strikes the similarity between the cluster spatial distribution for the 1979–1983 CZCS period (Figure 2a) and of the 1998–2010 SeaWiFS El Niño years (Figure 7b). Less evident, though still visible in particular in the Northwestern subtropical Pacific, is the correspondence between the 1998–2002 SeaWiFS period (Figure 1b) and the La Niña years (Figure 7a). Again, we interpret these patterns of the Transitional Bloom as an effect of the multiyear average, as during the CZCS period (1979–1983), a strong El Niño was detected, while during the 1982–2002 SeaWiFS years both El Niño and La Niña events are observed.

[58] Despite this, the expansion of the Transitional Bloom during 1998–2002 (which further intensifies if the whole 1998–2010 SeaWiFS period is considered) indicates that the change from 1979 to 1983 and 1998–2002 reflects a large scale change in the functioning of a part of the Northern Hemisphere, which could be related to the La Niña/El Niño effects. From a marked and geographically well defined seasonality, chlorophyll distribution changed to a much higher variability in time and space, which produces an overall smoothing of the seasonal patterns. Typical phytoplankton maxima of December–January in the Subtropical North and April–May in the Bloom regimes respectively flattens over a longer time interval (November–March), mostly reflecting a phase shift in space and time. In other words, the change in phenology does not occur coherently all over a given bioregion but with a patchy pattern.

[59] This change may have also been enhanced by the fact that spatial variability during CZCS might have been minimized by the averaging of a less frequent and spatially coarser coverage. Therefore, it is not possible to state if it reflects a long-term trend or just a variation at decadal scale. Certainly, it prompts for an in depth investigation on the possible link of the evident change in the seasonal cycle of phytoplankton chlorophyll with the functioning of the food web.

4.3. Final Considerations

[60] Analysis of ocean color data from the 1979–1983 and 1998–2002 indicates a modification of the phytoplankton phenological regimes in Northern Hemisphere temperate latitudes and in the equatorial belt. In particular, in subtropical areas of the North Pacific and Atlantic Oceans, we observed a widespread expansion of a regime showing a smoothing of seasonality (i.e., Transitional Bloom). A careful analysis of this expansion strongly suggests that the smoothing of the seasonal pattern is indeed linked to an increase of variability in the phase of seasonal cycle in space and time. This in turn suggests that the Transitional Bloom regime is not a new regime but the just the juxtaposition of the Subtropical North and Bloom regimes. The data do not allow for conclusive assessment of the causes–for example, whether these changes indicate coherent responses to a single large-scale forcing change and associated teleconnections. Nevertheless, identification of phenological clusters can help give insight into forcing mechanisms by manageably summarizing the huge volumes of information held in satellite data archives and by providing a synoptic, synthesizing view of the spatial distribution of phenological regimes. With further work, the observed phenological changes are likely to be attributable to changes in forcing mechanisms at local and global scales.

[61] While averaging satellite observations over several years highlights dominant modes of a long period and highlights differences, the analysis of years taken as single or grouped by two or three is also highly informative. Differently from the comparison of absolute chlorophyll concentrations, clustering of normalized concentration provides a synthetic view of the spatial response of phytoplankton to variation in, presumably, environmental conditions, which are reflected in a change in phenology.

[62] From our analysis it emerged that the main characteristics of large-scale ocean phytoplankton phenology (i.e., the relative magnitudes and timing of the four primary cycles) remained unaltered between the 1979–1983 and 1998–2002 years. Bloom, Tropical, Subtropical North, and Subtropical South regimes were all observed in the world's oceans during both time periods. Bioregions defined on the basis of phenological similarity did, however, change size and geographical distribution.

[63] In other words, as previously proposed by *Smayda* [1998], modification of physical forcing factors does not necessarily induce substantial modification of the typical, fundamental phytoplankton seasonal cycles. Instead, the spatial distribution of these typical seasonal cycles is altered when physical and biological conditions change. Understanding the relative roles of various forcing mechanisms in shaping phenological bioregions is a prerequisite to understanding the response of oceanic ecosystems to changing environmental conditions.

[64] Our results build on a large body of evidence that illustrates the key role of satellite ocean color observations in the long term monitoring of ocean ecosystems. The need to maintain a global ocean color record over decades [*McClain et al.*, 2004] is clear.

[65] **Acknowledgments.** We thank the anonymous reviewers, as well as Daniele Iudicone and Louis Prieur, for the comments they provided on this manuscript. We would like to specially thank Tonya Clayton. This work was performed within the framework of the *GLOBPHY* project, which was funded by the French *Agence Nationale de la Recherche* (ANR, Paris).

References

Antoine, D., A. Morel, H. R. Gordon, V. F. Banzon, and R. H. Evans (2005), Bridging ocean color observations of the 1980s and 2000s in search of long-term trends, *J. Geophys. Res.*, *110*, C06009, doi:10.1029/2004JC002620.

Banse, K., and C. R. McClain (1986), Satellite-observed winter blooms of phytoplankton in the Arabian Sea, *Mar. Ecol. Prog. Ser.*, *34*(3), 201–211, doi:10.3354/meps034201.

Beaugrand, G., F. Ibanez, and P. C. Reid (2000), Spatial, seasonal and long-term fluctuations of plankton in relation to hydroclimatic features in the English Channel, Celtic Sea and Bay of Biscay, *Mar. Ecol. Prog. Ser.*, *200*, 93–102, doi:10.3354/meps200093.

Beaugrand, G., P. C. Reid, F. Ibanez, J. A. Lindley, and M. Edwards (2002), Reorganization of North Atlantic marine copepod biodiversity and climate, *Science*, *296*(5573), 1692–1694, doi:10.1126/science.1071329.

Beaugrand, G., C. Luczak, and M. Edwards (2009), Rapid biogeographical plankton shifts in the North Atlantic Ocean, *Global Change Biol.*, *15*(7), 1790–1803, doi:10.1111/j.1365-2486.2009.01848.x.

Behrenfeld, M. J., et al. (2001), Biospheric primary production during an ENSO transition, *Science*, *291*(5513), 2594–2597, doi:10.1126/science.1055071.

Behrenfeld, M. J., E. Boss, D. A. Siegel, and D. M. Shea (2005), Carbon-based ocean productivity and phytoplankton physiology from space, *Global Biogeochem. Cycles*, *19*, GB1006, doi:10.1029/2004GB002299.

Behrenfeld, M. J., R. T. O'Malley, D. A. Siegel, C. R. McClain, J. L. Sarmiento, G. C. Feldman, A. J. Milligan, P. G. Falkowski, R. M. Letelier, and E. S. Boss (2006), Climate-driven trends in contemporary ocean productivity, *Nature*, *444*(7120), 752–755, doi:10.1038/nature05317.

Bograd, S. J., D. G. Foley, F. B. Schwing, C. Wilson, R. M. Laurs, J. J. Polovina, E. A. Howell, and R. E. Brainard (2004), On the seasonal and interannual migrations of the transition zone chlorophyll front, *Geophys. Res. Lett.*, *31*(17), L17204, doi:10.1029/2004GL020637.

Bond, N. A., J. E. Overland, M. Spillane, and P. Stabeno (2003), Recent shifts in the state of the North Pacific, *Geophys. Res. Lett.*, *30*(23), 2183, doi:10.1029/2003GL018597.

Boyce, D. G., M. R. Lewis, and B. Worm (2010), Global phytoplankton decline over the past century, *Nature*, *466*(7306), 591–596, doi:10.1038/nature09268.

Brock, J. C., and C. R. McClain (1992), Interannual variability in phytoplankton blooms observed in the northwestern Arabian Sea during the southwest monsoon, *J. Geophys. Res.*, *97*(C1), 733–750, doi:10.1029/91JC02225.

Brock, J. C., C. R. McClain, and W. W. Hay (1992), A southwest monsoon hydrographic climatology for the northwestern Arabian Sea, *J. Geophys. Res.*, *97*(C6), 9455–9465, doi:10.1029/92JC00813.

Carton, J. A., and B. S. Giese (2008), A reanalysis of ocean climate using Simple Ocean Data Assimilation (SODA), *Mon. Weather Rev.*, *136*(8), 2999–3017, doi:10.1175/2007MWR1978.1.

Carton, J. A., S. A. Grodsky, and H. Liu (2008), Variability of the oceanic mixed layer, 1960–2004, *J. Clim.*, *21*(5), 1029–1047, doi:10.1175/2007JCLI1798.1.

Cleland, E. E., I. Chuine, A. Menzel, H. A. Mooney, and M. D. Schwartz (2007), Shifting plant phenology in response to global change, *Trends Ecol. Evol.*, *22*(7), 357–365, doi:10.1016/j.tree.2007.04.003.

Conkright, M. E., and W. W. Gregg (2003), Comparison of global chlorophyll climatologies: In situ, CZCS, Blended in situ -CZCS and SeaWiFS, *Int. J. Remote Sens.*, *24*(5), 969–991, doi:10.1080/01431160110115573.

de Boyer Montégut, C., G. Madec, A. S. Fischer, A. Lazar, and D. Iudicone (2004), Mixed layer depth over the global ocean: An examination of profile data and a profile-based climatology, *J. Geophys. Res.*, *109*, C12003, doi:10.1029/2004JC002378.

Dessier, A., and J. R. Donguy (1994), The sea-surface salinity in the tropical Atlantic between 10°S and 30°N—Seasonal and interannual variations (1977–1989), *Deep Sea Res., Part I*, *41*(1), 81–100, doi:10.1016/0967-0637(94)90027-2.

Deuser, W. G., F. E. Mullerkarger, and C. Hemleben (1988), Temporal variations of particle fluxes in the deep subtropical and tropical North Atlantic: Eulerian versus Lagrangian effects, *J. Geophys. Res.*, *93*(C6), 6857–6862, doi:10.1029/JC093iC06p06857.

Devred, E., T. Platt, and S. Sathyendranath (2007), Delineation of ecological provinces using ocean colour radiometry, *Mar. Ecol. Prog. Ser.*, *346*, 1–13, doi:10.3354/meps07149.

Di Lorenzo, E., et al. (2008), North Pacific Gyre Oscillation links ocean climate and ecosystem change, *Geophys. Res. Lett.*, *35*(8), L08607, doi:10.1029/2007GL032838.

D'Ortenzio, F., and M. Ribera d'Alcalà (2009), On the trophic regimes of the Mediterranean Sea: A satellite analysis, *Biogeosciences*, *6*(2), 139–148, doi:10.5194/bg-6-139-2009.

Edwards, M., and A. J. Richardson (2004), Impact of climate change on marine pelagic phenology and trophic mismatch, *Nature*, *430*(7002), 881–884, doi:10.1038/nature02808.

Enfield, D. B., A. M. Mestas-Nunez, and P. J. Trimble (2001), The Atlantic multidecadal oscillation and its relation to rainfall and river flows in the continental US, *Geophys. Res. Lett.*, *28*(10), 2077–2080, doi:10.1029/2000GL012745.

Farmer, C. J. Q., T. A. Nelson, M. A. Wulder, and C. Derksen (2010), Identification of snow cover regimes through spatial and temporal clustering of satellite microwave brightness temperatures, *Remote Sens. Environ.*, *114*(1), 199–210, doi:10.1016/j.rse.2009.09.002.

Feldman, G., D. J. Clark, and D. Halpen (1984), Satellite color observations of the phytoplankton distribution in the eastern equatorial Pacific during the 1982–1983 El Nino, *Science*, *226*, 1069–1071, doi:10.1126/science.226.4678.1069.

Follows, M. J., and S. Dutkiewicz (2001), Meteorological modulation of the North Atlantic spring bloom, *Deep Sea Res., Part II*, *49*, 321–344, doi:10.1016/S0967-0645(01)00105-9.

Fovell, R. G. (1997), Consensus clustering of U.S. temperature and precipitation data, *J. Clim.*, *10*(6), 1405–1427, doi:10.1175/1520-0442(1997)010<1405:CCOUST>2.0.CO;2.

Gregg, W. W., M. E. Conkright, P. Ginoux, J. E. O'Reilly, and N. W. Casey (2003), Ocean primary production and climate: Global decadal changes, *Geophys. Res. Lett.*, *30*(15), 1809, doi:10.1029/2003GL016889.

Grodsky, S. A., J. A. Carton, and C. R. McClain (2008), Variability of upwelling and chlorophyll in the equatorial Atlantic, *Geophys. Res. Lett.*, *35*, L03610, doi:10.1029/2007GL032466.

Hartigan, J. H. (1975), *Clustering Algorithms*, 351 pp., Wiley, New York.

Hennig, C. (2007), Cluster-wise assesement of cluster stability, *Comput. Stat. Data Anal.*, *52*, 258–271, doi:10.1016/j.csda.2006.11.025.

Henson, S. A., J. P. Dunne, and J. L. Sarmiento (2009), Decadal variability in North Atlantic phytoplankton blooms, *J. Geophys. Res.*, *114*, C04013, doi:10.1029/2008JC005139.

Hovis, W. A., et al. (1980), Nimbus-7 Coastal Zone Color Scanner: System description and initial imagery, *Science*, *210*(4465), 60–63, doi:10.1126/science.210.4465.60.

Huber, V., R. Adrian, and D. Gerten (2008), Phytoplankton response to climate warming modified by trophic state, *Limnol. Oceanogr.*, *53*(1), 1–13, doi:10.4319/lo.2008.53.1.0001.

Hurrell, J. W. (1995), Decadal trends in the North Atlantic Oscillation: Regional temperatures and precipitation, *Science*, *269*(5224), 676–679, doi:10.1126/science.269.5224.676.

Ji, R., M. Edwards, D. L. Mackas, J. A. Runge, and A. C. Thomas (2010), Marine plankton phenology and life history in a changing climate: Current research and future directions, *J. Plankton Res.*, *32*, 1355–1368, doi:10.1093/plankt/fbq062.

Kromkamp, J. C., and T. Van Engeland (2010), Changes in phytoplankton biomass in the Western Scheldt estuary during the period 1978–2006, *Estuaries Coasts*, *33*(2), 270–285, doi:10.1007/s12237-009-9215-3.

Li, T. M., and S. G. H. Philander (1997), On the seasonal cycle of the equatorial Atlantic Ocean, *J. Clim.*, *10*(4), 813–817, doi:10.1175/1520-0442(1997)010<0813:OTSCOT>2.0.CO;2.

Li, Y., and N.-C. Lau (2012), Contributions of downstream eddy development to the teleconnection between ENSO and the atmospheric circulation over the North Atlantic, *J. Clim.*, *25*, 4993–5010, doi:10.1175/JCLI-D-11-00377.1.

Longhurst, A. (1995), Seasonal cycles of pelagic production and consumption, *Prog. Oceanogr.*, *36*, 77–167, doi:10.1016/0079-6611(95)00015-1.

Longhurst, A. R. (1998), *Ecological Geography of the Sea*, 552 pp., Elsevier Sci., New York.

Lund, R., and B. Li (2009), Revisiting climate region definitions via clustering, *J. Clim.*, *22*(7), 1787–1800, doi:10.1175/2008JCLI2455.1.

Mantua, N. J., and S. R. Hare (2002), The Pacific decadal oscillation, *J. Oceanogr.*, *58*(1), 35–44, doi:10.1023/A:1015820616384.

Mantua, N. J., S. R. Hare, Y. Zhang, J. M. Wallace, and R. C. Francis (1997), A Pacific interdecadal climate oscillation with impacts on salmon production, *Bull. Am. Meteorol. Soc.*, *78*(6), 1069–1079, doi:10.1175/1520-0477(1997)078<1069:APICOW>2.0.CO;2.

Marra, J., and R. T. Barber (2005), Primary productivity in the Arabian Sea: A synthesis of JGOFS data, *Prog. Oceanogr.*, *65*(2–4), 159–175, doi:10.1016/j.pocean.2005.03.004.

Martinez, E., D. Antoine, F. D'Ortenzio, and B. Gentili (2009), Climate-driven basin-scale decadal oscillations of oceanic phytoplankton, *Science*, *326*(5957), 1253–1256, doi:10.1126/science.1177012.

McClain, C. R. (2009), A decade of satellite ocean color observations, *Annu. Rev. Mar. Sci.*, *1*, 19–42, doi:10.1146/annurev.marine.010908.163650.

McClain, C. R., G. C. Feldman, and S. B. Hooker (2004), An overview of the SeaWiFS project and strategies for producing a climate research quality global ocean bio-optical time series, *Deep Sea Res., Part II*, *51*(1–3), 5–42, doi:10.1016/j.dsr2.2003.11.001.

McPhaden, M. J., T. Lee, and D. McClurg (2011), El Niño and its relationship to changing background conditions in the tropical Pacific Ocean, *Geophys. Res. Lett.*, *38*, L15709, doi:10.1029/2011GL048275.

Menzel, A., et al. (2006), European phenological response to climate change matches the warming pattern, *Global Change Biol.*, *12*(10), 1969–1976, doi:10.1111/j.1365-2486.2006.01193.x.

Monger, B., C. McClain, and R. Murtugudde (1997), Seasonal phytoplankton dynamics in the eastern tropical Atlantic, *J. Geophys. Res.*, *102*(C6), 12,389–12,491, doi:10.1029/96JC03982.

Moore, T. S., J. W. Campbell, and H. Feng (2001), A fuzzy logic classification scheme for selecting and blending satellite ocean color algorithms, *IEEE Trans. Geosci. Remote Sens.*, *39*(8), 1764–1776, doi:10.1109/36.942555.

Oliver, M. J., and A. J. Irwin (2008), Objective global ocean biogeographic provinces, *Geophys. Res. Lett.*, *35*, L15601, doi:10.1029/2008GL034238.

Pennington, J. T., K. L. Mahoney, V. S. Kuwahara, D. D. Kolber, R. Calienes, and F. P. Chavez (2006), Primary production in the eastern tropical Pacific: A review, *Prog. Oceanogr.*, *69*(2–4), 285–317, doi:10.1016/j.pocean.2006.03.012.

Penuelas, J., T. Rutishauser, and I. Filella (2009), Phenology Feedbacks on Climate Change, *Science*, *324*(5929), 887–888, doi:10.1126/science.1173004.

Pérez, V., E. Fernández, E. Marañón, P. Serret, and C. García-Soto (2005), Seasonal and interannual variability of chlorophyll *a* and primary production in the Equatorial Atlantic: *In situ* and remote sensing observations, *J. Plankton Res.*, *27*(2), 189–197, doi:10.1093/plankt/fbh159.

Peterson, W. T., and F. B. Schwing (2003), A new climate regime in northeast pacific ecosystems, *Geophys. Res. Lett.*, *30*(17), 1896, doi:10.1029/2003GL017528.

Platt, T., and S. Sathyendranath (2008), Ecological indicators for the pelagic zone of the ocean from remote sensing, *Remote Sens. Environ.*, *112*(8), 3426–3436, doi:10.1016/j.rse.2007.10.016.

Platt, T., G. N. White Iii, L. Zhai, S. Sathyendranath, and S. Roy (2009), The phenology of phytoplankton blooms: Ecosystem indicators from remote sensing, *Ecol. Modell.*, *220*(21), 3057–3069, doi:10.1016/j.ecolmodel.2008.11.022.

Platt, T., S. Sathyendranath, G. White, C. Fuentes-Yaco, L. Zhai, E. Devred, and C. Tang (2010), Diagnostic properties of phytoplankton time series from remote sensing, *Estuaries Coasts*, *33*(2), 428–439, doi:10.1007/s12237-009-9161-0.

Polovina, J. J., E. Howell, D. R. Kobayashi, and M. P. Seki (2001), The transition zone chlorophyll front, a dynamic global feature defining migration and forage habitat for marine resources, *Prog. Oceanogr.*, *49*(1–4), 469–483, doi:10.1016/S0079-6611(01)00036-2.

Racault, M. F., C. Le Quéré, E. Buitenhuis, S. Sathyendranath, and T. Platt (2012), Phytoplankton phenology in the global ocean, *Ecol. Indic.*, *14*, 152–163, doi:10.1016/j.ecolind.2011.07.010.

Radenac, M. H., F. Leger, A. Singh, and T. Delcroix (2012), Sea surface chlorophyll signature in the tropical Pacific during eastern and central Pacific ENSO events, *J. Geophys. Res.*, *117*, C04007, doi:10.1029/2011JC007841.

Ratkowsky, D. A., and G. N. Lance (1978), A criterion for determining the number of groups in a classification, *Aust. Comput. J.*, *10*, 115–117.

Riley, G. A. (1946), Factors controlling phytoplankton populations on Georges Bank, *J. Mar. Res.*, *6*, 54–73.

Sarmiento, J. L., et al. (2004), Response of ocean ecosystems to climate warming, *Global Biogeochem. Cycles*, *18*, GB3003, doi:10.1029/2003GB002134.

Schneider, N., and B. D. Cornuelle (2005), The forcing of the Pacific decadal oscillation, *J. Clim.*, *18*(21), 4355–4373, doi:10.1175/JCLI3527.1.

Siegel, D. A., S. C. Doney, and J. A. Yoder (2002), The North Atlantic Spring Phytoplankton bloom and Sverdrup's critical depth hypothesis, *Science*, *296*, 730–733, doi:10.1126/science.1069174.

Smayda, T. (1998), Patterns of variability characterizing marine phytoplankton, with examples from Narragansett Bay, *ICES J. Mar. Sci.*, *55*, 562–573, doi:10.1006/jmsc.1998.0385.

Strutton, P. G., W. Evans, and F. P. Chavez (2008), Equatorial Pacific chemical and biological variability, 1997–2003, *Global Biogeochem. Cycles*, *22*, GB2001, doi:10.1029/2007GB003045.

Tilburg, C. E., B. Subrahmanyam, and J. J. O'Brien (2002), Ocean color variability in the Tasman Sea, *Geophys. Res. Lett.*, *29*(10), 1487, doi:10.1029/2001GL014071.

Vargas, M., C. W. Brown, and M. R. P. Sapiano (2009), Phenology of marine phytoplankton from satellite ocean color measurements, *Geophys. Res. Lett.*, *36*, L01608, doi:10.1029/2008GL036006.

Wang, C., and P. C. Fiedler (2006), ENSO variability in the eastern tropical Pacific: A review, *Prog. Oceanogr.*, *69*(2–4), 239–266, doi:10.1016/j.pocean.2006.03.004.

Weeks, S. J., and F. A. Shillington (1994), Interannual scales of variation of pigment concentrations from Coastal Zone Color Scanner data in the Benguela Upwelling system and the subtropical Convergence Zone south of Africa, *J. Geophys. Res.*, *99*(C4), 7385–7399, doi:10.1029/93JC02143.

Winder, M., and D. E. Schindler (2004), Climatic effects on the phenology of lake processes, *Global Change Biol.*, *10*(11), 1844–1856, doi:10.1111/j.1365-2486.2004.00849.x.

Wolter, K., and M. S. Timlin (2011), El Nino/Southern Oscillation behaviour since 1871 as diagnosed in an extended multivariate ENSO index (MEI.ext), *Int. J. Climatol.*, *31*(7), 1074–1087, doi:10.1002/joc.2336.

Yoder, J. A., C. R. McClain, G. C. Feldman, and W. E. Esaias (1993), Annual cycles of phytoplankton chlorophyll concentrations in the global ocean - a satellite view, *Global Biogeochem. Cycles*, *7*(1), 181–193, doi:10.1029/93GB02358.